Maximum Throughput Path Selection With Random Blockage for Indoor 60 GHz Relay Networks

Guang Yang, *Student Member, IEEE*, Jinfeng Du, *Member, IEEE*, and Ming Xiao, *Senior Member, IEEE*

Abstract—Indoor communications in the 60 GHz band is capable of supporting multi-gigabit wireless access thanks to the abundant spectrum and the possibility of using dense antenna arrays. However, the high directivity and penetration loss make it vulnerable to blockage events, which can be frequent in indoor environments. Given network topology information in sufficient precision, we investigate the average throughput and outage probability when the connection between any two nodes can be established either via the *line-of-sight* (LOS) link, through a reflection link, or by a half-duplex relay node. We model the reflection link as an LOS with extra power loss and derive the closed-form expression for the relative reflection loss. For networks with a central coordinator and multiple relays, we also propose a generic algorithm, *maximum throughput path selection* (MTPS), to select the optimal path that maximizes the throughput. The complexity of the MTPS algorithm is $\mathcal{O}(n^2)$ for networks equipped with n relays, whereas a brute-forced algorithm has complexity of $\mathcal{O}(n \cdot n!)$. Numerical results show that increasing the number of relays can significantly increase the average throughput and decrease the outage probability, and resorting to reflection paths provides significant gains when the probability of link blockage is high.

Index Terms—60 GHz, relay, reflection, blockage, throughput, outage.

I. INTRODUCTION

WIRELESS communications in the 60 GHz band can provide multi-gigabit short-range wireless access in indoor environments, such as the Wireless Gigabit Alliance (WiGig) technology [1], thanks to the abundant spectrum and high power gain antenna arrays. The high directional antennas and high penetration loss can greatly reduce the power of interfering signals but at the same time make it vulnerable to blockage events. Connectivity and throughput can be seriously impaired by blockage owing to the extremely weak capability of penetration and diffraction for 60 GHz radio waves [2]–[6], which is due to the physical property of radios with very short wavelength. As such blockage events may happen frequently due to object mobility (e.g., the movement of a human body), it is challenging to provide multi-gigabit throughput while reducing the outage probability to a sufficiently low level.

Numerous efforts devoted to 60 GHz communications focus on various approaches to tackle the problem of blockage. We only provide a small sample of previous contributions here and readers are kindly referred to [7]–[9] for more comprehensive reviews on 60 GHz communications systems.

A large amount of experiments have been performed in [10]–[14] to characterize the property of indoor blockage events and their effect on signal strength by obstacle physical properties, such as size, shape, position, placement and density. The link blockage caused by random human activities has been analysed in [15] for typical indoor environments and in [16] in the context of 60 GHz wireless personal area networks (WPANs). One way to tackle the problem of link blockage and improve the robustness of indoor networks is to deploy relays. A pyramid relaying system proposed in [17] shows superior coverage and capacity under various human shadowing densities. Significant reduction of the path loss demonstrated in [18] reveals the importance of relay placement in improving the connectivity of 60 GHz indoor communications. The outage performance of decode-and-forward (DF) and amplify-and-forward (AF) relaying in [19] is analyzed by taking co-channel interference into account. On the other hand, the feasibility of data transmission via the first-order reflected radio waves has been verified in [5], [20] where no *line-of-sight* (LOS) path exists and the path loss is high. Two beam switching strategies proposed in [21] switch the beam path from LOS link to a *non-line-of-sight* (NLOS) link to resolve the link blockage. It is further demonstrated in [22] that beamforming and beam combining techniques can be beneficial to significantly increase the SNR for the NLOS transmissions. Since reflection comes with almost no extra cost, it is valuable to evaluate and quantify its benefit as a complementary component of actively deployed relay nodes.

For multi-hop LOS transmissions, an optimal geographic routing protocol is proposed in [23] and a link scheduling scheme for 60 GHz multi-channel wireless mesh networks is investigated in [24]. A routing algorithm is developed in [25] to find the optimal relay path with the least interference to maximize the throughput. With high directional antennas, a multi-hop LOS relaying protocol proposed in [16] achieves high network utilization with low overhead despite high link

blockage probability in a 60 GHz indoor WPAN. The robustness of routing schemes is discussed in [26] and neighbor discovery protocols are proposed in [27] to improve the signal quality and maintain the connectivity. A randomized exclusive region based scheduling scheme is proposed in [28] to explore the potentials of spatial reuse, and the benefit of multi-hop concurrent transmissions is investigated in [29] for networks with linearly deployed nodes and no link blockage.

In this paper, we consider an indoor 60 GHz relay network where the connection between any two user nodes can be established either via the LOS link, through a reflection link, or by a half-duplex relay node. We focus on scenarios where the network has a central coordinator and multiple half-duplex relay nodes deployed as a fixed infrastructure. We assume all devices (including relays and user nodes) are equipped with directional antennas and their topology can be measured with sufficient precision [30]–[32]. Given the topology information of distance and direction, we investigate how such topology information can be used to improve the system performance. Because the small-scale multipath effect in 60 GHz communications is negligible [5], [6], the data rate supported by a specific link is determined by the transmit power, antenna gains, pass loss exponent and the transmission distance. By modeling the reflection link as an LOS transmission with extra power loss, we can calculate the throughput of each of the three options, namely, the LOS link, the reflection link, and the relay link. We investigate the average throughput and the outage probability under two random blockage models where the probability of blockage is identical for all links (topology independent) or is proportional to the length of the link (topology dependent). We propose the *maximum throughput path selection* (MTPS) algorithm with low complexity for multi-relay scenarios to select the best path that consists of one or more hops to maximize the throughput when the knowledge of blockage events is available.

To highlight our objective, we do not consider the combining of signals from different propagation paths. Although the extension of our analysis to scenarios with multiple propagation paths can be straightforward via approaches such as beam combining [22], the extension based on radio wave broadcast via a single beam is highly non-trivial due to the high directivity of 60 GHz antenna arrays. Besides, we do not take into account the interference from concurrent transmissions when multiple relays are selected to assist transmission for the following two reasons. Firstly, the communicating nodes (users and relays) in our network are deployed inside a hall in contrast to the linear deployment in [28], [29], and therefore the probability that concurrent transmissions fall into the boresight scenario at the same receiving node at the same time (hence causing severe interference) is very small given the high directivity of antenna arrays and the random positions of the communicating nodes. Secondly, the effect of interference from concurrent transmissions can be partially modeled by link blockage events since severely degraded link quality can be treated as link blockage.

Our study differs from the existing results from the following aspects:

- The routing schemes in [23]–[25], [28], [29] do not consider the link blockage, while the main objective of

our study is to develop a routing algorithm for the network with link blockage;
- In [17]–[19] the performance is studied for 60 GHz relaying channels. Yet, they only consider fixed relaying networks with 2 hops and do not optimize relaying paths. We focus on generic routing schemes including hop selection and reflection utilization such that the throughput can be maximized in multi-hop networks;
- Although the approaches on reflection signals in [15], [16], [20], [21], [26], [27] are viable to maintain the link connectivity when the LOS channel is blocked, they are based on measured results. There is no closed-form analysis on 60 GHz reflection signals yet;
- For the multi-hop concurrent transmission (MHCT) proposed in [28], [29], the application scenarios are limited to nodes deployed in one line. In our framework nodes can be arbitrarily placed. Moreover, MHCT in [28], [29] does not consider the link blockage problem, whereas our schemes are mainly proposed to address the problem of link blockage.

The rest of the paper is organized as follows. We present the system model in Section II along with preliminaries on the reflection loss and relaying strategy. We investigate the average throughput and outage probability based on two random blockage models in Section III, and present the MTPS algorithm in Section IV. Our models and analysis are validated by numerical results in Section V and conclusions are given in Section VI.

II. SYSTEM MODEL AND ADAPTIVE RELAYING SCHEME

A. Link Model and Network Architecture

Given the transmit power P_t, the transmitter antenna gain G_t, and the receiver antenna gain G_r, the power of the received signals can be determined as follows:

$$P_r(l) = P_t G_t G_r \left(\frac{\lambda}{4\pi}\right)^2 \left(\frac{1}{l}\right)^n, \tag{1}$$

where λ is wavelength, l is the transmission distance, and n is the path loss exponent which ranges from 2 to 6 from 60 GHz measurement in [5]. Note that (1) is a modified version of the standard Friis free space transmission equation in which the path loss exponent is $n = 2$. However, in practical situations the path loss exponent n in the empirical and deterministic model (1) can be higher due to shadowing and oxygen absorption. Given system bandwidth W and one-side power spectral density of white Gaussian noise N_0, the achievable[1] rate is given by

$$R(l) = W \log_2(1 + \alpha l^{-n}), \tag{2}$$

where $\alpha = \frac{P_t G_t G_r \lambda^2}{16\pi^2 N_0 W}$ represents the signal-to-noise ratio (SNR) measured at $l = 1$ meter distance. To simplify notations, we assume that all transmission links have the same α, and extensions to general setups are straightforward.

---

[1]Strictly speaking, the rate in (2) is actually the capacity, i.e., the theoretical upper bound on data rate that may be achieved asymptotically.
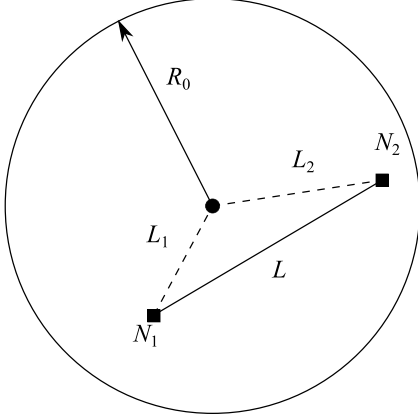
Fig. 1. Randomly distributed nodes in a circular space, where the relay node is placed at the center and two communicating user nodes N_1 and N_2 are randomly located in the hall with radius R_0.

Fig. 2. The LOS path between a transmitter N_1 at (x_1, y_1) and a receiver N_2 at (x_2, y_2), and a reflection path via the surface on the x-axis. N_1' at $(x_1, -y_1)$ is a mirror node of N_1 w.r.t. the reflection surface, θ is the incident angle, l and l' are the distances of the LOS link and reflection, respectively.

We consider a 60 GHz wireless relay network where a pair of communication nodes N_1 and N_2 are randomly placed within a circular space, as shown in Fig. 1, with the center C and radius R_0. One or more half-duplex relay nodes are deployed inside this area to assist transmission. Supposing N_1 and N_2 are uniformly distributed in the circular area, and their distances to the center C, denoted by L_1 and L_2, respectively, are random variables with a probability density function (p.d.f.)

$$f_{L_i}(l_i) = \frac{2l_i}{R_0^2}, \text{ where } 0 < l_i < R_0 \text{ and } i = 1, 2. \quad (3)$$

The distance between N_1 and N_2, denoted as L, follows the p.d.f. [33]:

$$f_L(l) = \frac{2l}{R_0^2} \left[1 - \frac{2}{\pi} \arcsin\left(\frac{l}{2R_0}\right) - \frac{l}{\pi R_0}\sqrt{1 - \frac{l^2}{4R_0^2}} \right], \quad (4)$$

where $0 < l < 2R_0$.

The LOS link between any two nodes may be blocked by an obstacle (e.g., human body) in indoor scenarios. We further assume that the reflection path between any two nodes is always available [14], since such reflection may happen via the floor, the ceiling, or walls.[2]

We further assume that the network has a central coordinator installed to take care of the synchronization and management of the network information. It collects and updates necessary information, manages the path selection process, and coordinates the communications according to an optimized scheduling. Such central coordinator can be realized, for example, in the form of a piconet coordinator as suggested by [32] for the high rate WPAN, or by the access point that connects the indoor network with other networks. We will discuss the operation of the central coordinator, its status update process, and the associated overhead in Section IV.
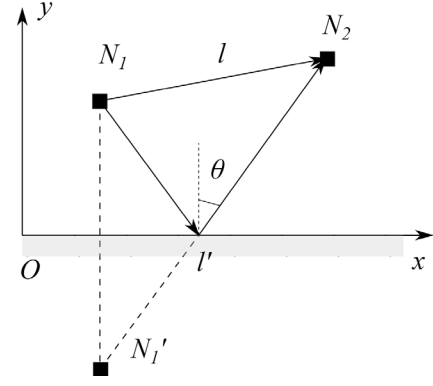
---

[2]Given a single beam at the transmitter and the receiver, there is only one feasible reflection path due to the high directivity of 60 GHz antenna arrays.

B. Relative Reflection Loss

In indoor scenarios, signals from the reflection path suffer from extra path loss compared to LOS signals due to the extended transmission distance and the power loss on the surface of reflective materials. The attenuation from reflection depends on the material thickness, permittivity, and the incident angle [34]. The power of the first-order reflected wave is (in total) about 15 dB lower than that of the LOS wave [5], [20]. Despite of the power loss, wave reflection from the ceiling has been proven to be a viable way of preserving connectivity and avoiding blockage [14].

Definition 1 (Relative Reflection Loss): The *relative reflection loss* χ is defined as the extra power attenuation experienced by the reflection path compared to the LOS path. That is, denoting P_{LOS} and $P_{\text{reflection}}$ (L_{LOS} and $L_{\text{reflection}}$) as the received power in decibel (path loss in dB) for the LOS link and reflection link, respectively, we have

$$\chi = P_{\text{LOS}} - P_{\text{reflection}} = L_{\text{reflection}} - L_{\text{LOS}} \text{ [dB]}.$$

Proposition 1: Let l and l' be the length of LOS path $N_1 \to N_2$ and reflection path $N_1' \to N_2$, respectively, as shown in Fig. 2, the *relative reflection loss* is given by

$$\chi(l, l', \theta) = 10n \log \frac{l'}{l} - 20 \log |\eta(\theta)| \text{ [dB]}, \quad (5)$$

where n is the path loss exponent, and θ denotes the incident angle, and $\eta(\theta)$ is the reflection coefficient given by [35]

$$\eta(\theta) = \frac{-\omega \cos \theta + \sqrt{\omega - \sin^2 \theta}}{\omega \cos \theta + \sqrt{\omega - \sin^2 \theta}}, \quad (6)$$

where ω is dielectric constant determined by the inherent physical property of reflective material.

Proof: See Appendix A for the proof. □

To validate our model for the relative reflection loss, we present in Table I the theoretical values of χ given by (5) and the measurement data χ^* based on the experimental results from [20], where the transmitter and the receiver are placed at the same horizontal plane (1 meter above the ground) in a

TABLE I
THE RELATIVE REFLECTION LOSS: χ OBTAINED FROM (5) VERSUS χ^*
CALCULATED BASED ON THE MEASUREMENT DATA IN [20]

Reflection	$\left(l, l', \theta\right)$	χ^*(dB)	χ(dB)
ceiling	$\left(2, 2\sqrt{5}, \arctan\left(\frac{1}{2}\right)\right)$	15.29	15.24
outer wall	$\left(2, 2\sqrt{10}, \arctan\left(\frac{1}{3}\right)\right)$	17.08	17.77
inner wall	$\left(2, 2\sqrt{10}, \arctan\left(\frac{1}{3}\right)\right)$	21.63	22.52
ground	$\left(2, 2\sqrt{2}, \frac{\pi}{4}\right)$	31.62	31.83

3-meter high empty room. The theoretical results match the measurement results to a good precision, which enables us to estimate the data rate via reflection paths based on the topology information. For the special case where the transmitter and the receiver have the same fixed distance to the reflection plane, $\chi(l, l', \theta)$ in (5) degenerates to $\chi(l)$ and the rate of the reflection path can be written as

$$R_{\text{refl}}(l) = W \log_2 \left(1 + \frac{\alpha}{\chi(l)} l^{-n}\right). \tag{7}$$

C. Optimized Time Splitting of Half-Duplex Relaying

Definition 2 (Optimized Time Splitting): Given a time slot, the *optimized time splitting* provides the time allocation between reception and transmission phases for the half-duplex DF relaying that maximizes the throughput.

Denoting $\beta \in (0, 1)$ the normalized time splitting parameter for relaying, the maximum throughput of a two-hop relay path is therefore

$$R_{\text{relay}}(l_1, l_2) = \max_{\beta \in (0,1)} \min \{\beta R(l_1), (1-\beta)R(l_2)\}, \tag{8}$$

where l_1 and l_2 are the length of two hops respectively.

Proposition 2: Let non-negative $R_1 = R(l_1)$ and $R_2 = R(l_2)$ represent the rates in two hops with transmission distance l_1 and l_2, respectively, the maximum throughput of the two-hop relaying is given by

$$R_{\text{relay}}(l_1, l_2) = \rho(R_1, R_2) \triangleq \begin{cases} 0, & \text{if } R_1 R_2 = 0, \\ \frac{R_1 R_2}{R_1 + R_2}, & \text{otherwise.} \end{cases} \tag{9}$$

Proof: (8) is maximized when $\beta R_1 = (1-\beta)R_2$, i.e., when $\beta = R_2/(R_1 + R_2)$, which leads to (9). $\square$

D. Relay-Prioritized Region and Critical Distance

Definition 3 (Relay-Prioritized Region): Relay-prioritized region is the region (of the circular space) in which relaying can provide higher transmission rate than the LOS path.

With half-duplex relaying, denoting l, l_1, l_2 the length of the LOS path and the two relaying paths, respectively, the relay-prioritized region exists if and only if

$$\rho(R(l_1), R(l_2)) > R(l), \tag{10}$$

for some $l_1, l_2 > 0$ and $l_1 + l_2 \geq l$. Note that the relay-prioritized region may not exist if the distance between the transmitter and the receiver is too close. To study the existence of the region, we have following definition.

Definition 4 (Critical Distance): Critical distance is the minimum distance between a pair of nodes for the existence of the relay-prioritized region.

Proposition 3: Given α and the path loss exponent n, the relay-prioritized region exists if and only if

$$l \geq l^* \triangleq \sqrt[n]{\frac{\alpha}{2^n - 2}}, \tag{11}$$

where l is the communication distance and l^* is the critical distance.

Proof: Since $R(l)$ defined by (2) is a monotonically decreasing function of l, the left-hand side of (10) is maximized when $l_1 = l_2 = l/2$. Substituting this into (10) and combining it with (2), we obtain the critical distance shown in (11). $\square$

The critical distance l^* decreases as n increases. As the path loss gets severer, it is more likely that a random deployed relay nodes can improve the throughput. Hence we can benefit more from utilizing relays in high path loss environments, compared to those with smaller n.

III. AVERAGE THROUGHPUT AND OUTAGE PROBABILITY

In contrast to the broadcasting wave propagation in lower frequency radios with omnidirectional antennas, the high directivity of 60 GHz antenna arrays changes the wave propagation characteristic significantly. In the boresight scenario, the received signal strength can be several order of magnitude higher than that of off-boresight scenarios. As a consequence, the communication between two nodes in an indoor environment as considered in Fig. 2 can only be established either via the LOS link of length l, the reflection path (e.g., via the ceiling) of length l', or via a half-duplex DF relaying node.

To quantify the benefits of using relaying and/or reflection, we investigate the average throughput and outage performance for the following four scenarios:

- Case I (LOS): only LOS link is available;
- Case II (LOS, Relay): both LOS and relay paths are available;
- Case III (LOS, Reflection): both LOS and reflection paths are available;
- Case IV (LOS, Relay, Reflection): LOS, relay, and reflection are available.

We start the analysis with a single relay, and then extend the results to multiple-relay scenarios.

A. Random Blockage Models

When a transmission path is blocked, the strength of the received signal will be severely degraded. For simplicity we assume that the transmission rate drops to zero once the link is blocked, and we call such an event the *link blockage*. The probability of blockage for a specific link depends on many aspects, such as the area of indoor space, the beamwidth of antenna array, the size/shape of obstacles, and the link length. To model the link blockage events, we assume that there are N obstacles that behave independently and randomly. Each

obstacle can block a link with probability p. That is, on average there are totally Np obstacles blocking some links. Here we consider two random blockage models, topology-independent and topology-dependent, that are described as follows. Given M links, labeled by $k = 1, \ldots, M$, if a link blockage event has occurred, the probability that link k is blocked in the topology-independent model is given by

$$\tau_k \triangleq \mathbb{P}(\text{link } k \text{ blocked} \mid \text{a link blockage}) = \frac{1}{M}, \qquad (12)$$

and in the topology-dependent model, we instead have

$$\tau_k = \frac{l_k}{l_s}, \quad \text{where } l_s \triangleq \sum_{k=1}^{M} l_k, \qquad (13)$$

and l_k is the length of link k. This is, in the topology-dependent model an active obstacle may block any link with probability proportional to the length of the link, which is motivated by the fact that the longer links are more likely to be blocked.

Therefore, the probability that link k is blocked is given by

$$p_k = \tau_k \mathbb{P}(\text{a link blockage occurs}) = \tau_k p, \qquad (14)$$

where $p = \sum_k p_k$ is the *link blockage probability* (or blockage probability in short). Note that each active obstacle cannot cause more than one link blockage at a time, unless it rightly stands in the area of the intersection of multiple links, where the area of intersected links depends on the beam-width. Here, the case of a single obstacle blocking multiple links is not considered in our model, since the probability of such events, which can be approximated by the ratio of the intersected area to the whole area of consideration, is much smaller than the probability given by (14), especially for the scenarios with narrow beamwidth. Yet, we will consider the scenario in which multiple obstacles may obstruct the same link simultaneously.

Supposing the nodes are randomly placed within a circular hall, as illustrated in Fig. 1, we first analyze the blockage probability (14) of each possible link based on the associated distance vector $\mathbf{L}$. The performance in terms of average throughput and outage probability are then evaluated by taking average over all possible $\mathbf{L}$. If no relay is deployed, the distance vector $\mathbf{L} = \{l\}$ contains only one element l whose distribution is given by (4). For the cases with one relay, we have $\mathbf{L} = \{l, l_1, l_2\}$, where l_1 and l_2 follow the marginal distribution given by (3). Note that l, l_1 and l_2 are not independent.

B. Average Throughput With Random Blockage

For the single relay scenario with distance vector $\mathbf{L} = \{l, l_1, l_2\}$, we denote A_1 as the number of obstacles in the LOS link (length l) and A_2 the number of obstacles in the relaying path (consisting of two links with length l_1 and l_2). To simplify the notation, we denote B_1 the event that the LOS link is blocked and B_2 the event that the relaying path is blocked. Thus, $A_i = 0$ implies that the corresponding path is available (indicated by $\bar{B}_i$); otherwise it is blocked (indicated by B_i). Since the relay path consists of two hops and obstacles on either hop will block the relying path, the blockage event B_2

for the relay path can be decomposed into two sub-events $B_2 = B_2^{(1)} \cup B_2^{(2)}$.

1) Case I (LOS): Since $\mathbf{L} = \{l\}$, we have $\tau_0 = 1$. Thus $p_0 = p$. The probability of no blockage is

$$\mathbb{P}\{\bar{B}_1\} = \mathbb{P}\{A_1 = 0\} = (1 - p)^N. \qquad (15)$$

Therefore we obtain the average throughput:

$$\bar{R}_{\mathrm{I}}(p) = \mathbb{E}\left[R(l)\right] \mathbb{P}\{\bar{B}_1\} = (1 - p)^N \mathbb{E}\left[R(l)\right], \qquad (16)$$

where $\mathbb{E}[R(l)]$ denotes the expectation over l.

2) Case II (LOS, Relay): Since $\mathbf{L} = \{l, l_1, l_2\}$, we have $p_k = \tau_k p$, $k = 0, 1, 2$. Only if both LOS and relay path are blocked, the connection between the transmitter and the receiver is lost. Based on path availability, the throughput can be analyzed for four circumstances as follows:

(1) If both LOS and relay path are available, we have

$$\mathbb{P}\{E_1 | \mathbf{L}\} \triangleq \mathbb{P}\{\bar{B}_1 \cap \bar{B}_2\} = (1 - p)^N. \qquad (17)$$

Since the transmitter-receiver pair can choose either path for communication, the maximum throughput is obtained as $R_{\max}^{(1)} = \max\{R(l), \rho(R(l_1), R(l_2))\}$.

(2) If the only relaying path is not blocked, we have

$$\mathbb{P}\{E_2 | \mathbf{L}\} \triangleq \mathbb{P}\{B_1 \cap \bar{B}_2\}$$
$$= \sum_{n=1}^{N} \mathbb{P}\left\{\sum_{i=1}^{2} A_i = n\right\} \mathbb{P}\left\{A_2 = 0 \,\middle|\, \sum_{i=1}^{2} A_i = n\right\}$$
$$= \sum_{n=1}^{N} \binom{N}{n} p_0^n (1 - p)^{N-n}$$
$$= \left[1 - (1 - \tau_0)p\right]^N - (1 - p)^N, \qquad (18)$$

and the corresponding rate is $R_{\max}^{(2)} = \rho(R(l_1), R(l_2))$.

(3) If only LOS is not block, the probability is

$$\mathbb{P}\{E_3 | \mathbf{L}\} \triangleq \mathbb{P}\{\bar{B}_1 \cap B_2\}$$
$$= \sum_{n=1}^{N} \mathbb{P}\left\{\sum_{i=1}^{2} A_i = n\right\} \mathbb{P}\left\{A_1 = 0 \,\middle|\, \sum_{i=1}^{2} A_i = n\right\}$$
$$= \sum_{n=1}^{N} \binom{N}{n} (p_1 + p_2)^n (1 - p)^{N-n}$$
$$= (1 - \tau_0 p)^N - (1 - p)^N, \qquad (19)$$

and the corresponding rate is $R_{\max}^{(3)} = R(l)$.

(4) If both LOS and relay paths are blocked, we have $R_{\max}^{(4)} = 0$ with the probability

$$\mathbb{P}\{E_4 | \mathbf{L}\} \triangleq \mathbb{P}\{B_1 \cap B_2\}$$
$$= 1 - \mathbb{P}\{\bar{B}_1 \cap \bar{B}_2\} - \mathbb{P}\{B_1 \cap \bar{B}_2\} - \mathbb{P}\{\bar{B}_1 \cap B_2\}. \qquad (20)$$

TABLE II
THROUGHPUT AND PROBABILITY OF ALL POSSIBLE BLOCKAGE EVENTS FOR CASE IV (LOS, RELAY, REFLECTION)

Blockage Event E_i $\mathbf{L}$	Maximum Rate $R_{\max}^{(i)}$	Conditional Probability $\mathbb{P}\{E_i\|\mathbf{L}\}$
$\bar{B}_1 \cap \bar{B}_2^{(1)} \cap \bar{B}_2^{(2)}$	$\max\{R(l),\ \rho(R(l_1), R(l_2))\}$	$(1-p)^N$
$\bar{B}_1 \cap B_2^{(1)} \cap \bar{B}_2^{(2)}$	$\max\{R(l),\ \rho(R_{\mathrm{refl}}(l_1), R(l_2))\}$	$(1-(1-\tau_1)p)^N - (1-p)^N$
$\bar{B}_1 \cap \bar{B}_2^{(1)} \cap B_2^{(2)}$	$\max\{R(l),\ \rho(R(l_1), R_{\mathrm{refl}}(l_2))\}$	$(1-(1-\tau_2)p)^N - (1-p)^N$
$\bar{B}_1 \cap B_2^{(1)} \cap B_2^{(2)}$	$\max\{R(l),\ \rho(R_{\mathrm{refl}}(l_1), R_{\mathrm{refl}}(l_2))\}$	$(1-\tau_0 p)^N + (1-p)^N - \left[(1-(1-\tau_1)p)^N + (1-(1-\tau_2)p)^N\right]$
$B_1 \cap \bar{B}_2^{(1)} \cap \bar{B}_2^{(2)}$	$\max\{R_{\mathrm{refl}}(l),\ \rho(R(l_1), R(l_2))\}$	$(1-(1-\tau_0)p)^N - (1-p)^N$
$B_1 \cap \bar{B}_2^{(1)} \cap B_2^{(2)}$	$\max\{R_{\mathrm{refl}}(l),\ \rho(R(l_1), R_{\mathrm{refl}}(l_2))\}$	$(1-\tau_1 p)^N + (1-p)^N - \left[(1-(1-\tau_0)p)^N + (1-(1-\tau_2)p)^N\right]$
$B_1 \cap B_2^{(1)} \cap \bar{B}_2^{(2)}$	$\max\{R_{\mathrm{refl}}(l),\ \rho(R_{\mathrm{refl}}(l_1), R(l_2))\}$	$(1-\tau_2 p)^N + (1-p)^N - \left[(1-(1-\tau_0)p)^N + (1-(1-\tau_1)p)^N\right]$
$B_1 \cap B_2^{(1)} \cap B_2^{(2)}$	$\max\{R_{\mathrm{refl}}(l),\ \rho(R_{\mathrm{refl}}(l_1), R_{\mathrm{refl}}(l_2))\}$	$1 + (1-p)^N - \sum_{i=0}^{2}\left[(1-\tau_i p)^N + (1-(1-\tau_i)p)^N\right]$

Thus, the throughput of Case II (LOS, Relay) for a given distance vector $\mathbf{L}$ is

$$\mathbb{E}\left[R_{\mathrm{II}}(p)|\mathbf{L}\right] = \sum_{i=1}^{4} R_{\max}^{(i)}\mathbb{P}\{E_i|\mathbf{L}\}, \qquad (21)$$

and the average throughput is obtained by averaging over all the possible realizations of $\mathbf{L} = \{l, l_1, l_2\}$, i.e.,

$$\bar{R}_{\mathrm{II}}(p) = \iiint\limits_{(l,l_1,l_2)} \mathbb{E}\left[R_{\mathrm{II}}(p)|\mathbf{L}\right] f_{\mathbf{L}}(l, l_1, l_2) dl dl_1 dl_2, \quad (22)$$

where $f_{\mathbf{L}}(l, l_1, l_2)$ is the joint probability distribution function.

3) Case III (LOS, Reflection): Due to the extra power loss by reflection, the reflection path will not be used unless the LOS is blocked. Thus the average throughput is

$$\bar{R}_{\mathrm{III}}(p) = \mathbb{E}\left[R(l)\right]\mathbb{P}\{\bar{B}_1\} + \mathbb{E}\left[R_{\mathrm{refl}}(l)\right]\mathbb{P}\{B_1\} \qquad (23)$$
$$= (1-p)^N \mathbb{E}\left[R(l)\right] + \left[1 - (1-p)^N\right]\mathbb{E}\left[R_{\mathrm{relf}}(l)\right],$$

which indicates that, when $\bar{R}_{\mathrm{I}}(p)$ approaches zero, there is still extra $\mathbb{E}[R_{\mathrm{relf}}(l)]$ provided by transmission via reflection.

4) Case IV (LOS, Relay, Reflection): The analysis is similar to in Case II (LOS, Relay), except that reflection is now taken into account. We can enumerate all the random blockage events and their corresponding throughput, and the results $(P\{E_i|\mathbf{L}\}, R_{\max}^{(i)})$ are summarized in Table II. Hence, the average throughput is

$$\bar{R}_{\mathrm{IV}}(p) = \iiint\limits_{(l,l_1,l_2)} \mathbb{E}\left[R_{\mathrm{IV}}(p)|\mathbf{L}\right] f_{\mathbf{L}}(l, l_1, l_2) dl dl_1 dl_2, \qquad (24)$$

where $\mathbb{E}[R_{\mathrm{IV}}(p)|\mathbf{L}]$ is given by

$$\mathbb{E}\left[R_{\mathrm{IV}}(p)|\mathbf{L}\right] = \sum_{i=1}^{8} R_{\max}^{(i)}\mathbb{P}\{E_i|\mathbf{L}\}. \qquad (25)$$

The extension to the multiple-relay scenario is straightforward and similar to the single-relay case.

C. Outage Probability with Random Blockage

Given a threshold rate R_ϵ, we say an outage event happens if the rate R is lower than R_ϵ. Thus the outage probability is

$$\mathbb{P}_{\mathrm{out}}(R_\epsilon) = \mathbb{P}\{R < R_\epsilon\}. \qquad (26)$$

Take Case II (LOS, Relay) for example. Given blockage probability p, the outage probability $\mathbb{P}\{R_{\mathrm{II}}(p) < R_\epsilon\}$ is a function of p that can be written as

$$\iiint\limits_{(l,l_1,l_2)} \mathbb{P}\{R_{\mathrm{II}}(p) < R_\epsilon|\mathbf{L}\} f_{\mathbf{L}}(l, l_1, l_2) dl dl_1 dl_2, \qquad (27)$$

where $\mathbb{P}\{R_{\mathrm{II}} < R_\epsilon|\mathbf{L}\}$ is the outage probability for given $\mathbf{L}$ and averaged over all the four different scenarios, i.e.,

$$\mathbb{P}\{R_{\mathrm{II}}(p) < R_\epsilon|\mathbf{L}\} = \sum_{i=1}^{4} \mathbb{P}\left\{R_{\max}^{(i)} < R_\epsilon\right\}\mathbb{P}\{E_i|\mathbf{L}\}, \qquad (28)$$

where $\mathbb{P}\{E_i \mid \mathbf{L}\}$ is the probability of the corresponding event E_i given $\mathbf{L}$, and it is different for the topology-independent or topology-dependent models.

To gain more insights of the outage performance, we set the threshold R_ϵ to a sufficiently low value such that the transmission rates of LOS or by the relay path are still above the threshold even if the terminals are the farthest apart. Thus, $\mathbb{P}\{R_{\max}^{(i)} < R_\epsilon\} = 0$, for $i = 1, 2, 3$, and $\mathbb{P}\{R_{\mathrm{II}}(p) < R_\epsilon \mid \mathbf{L}\} = \mathbb{P}\{E_4 \mid \mathbf{L}\}$. The outage probability is

$$\mathbb{P}_{\mathrm{out}}^{(\mathrm{1\_relay})}(p) = \iiint\limits_{(l,l_1,l_2)} \mathbb{P}\{E_4 \mid \mathbf{L}\} \cdot f_{\mathbf{L}}(l, l_1, l_2) dl dl_1 dl_2$$

$$= 1 - \iiint\limits_{(l,l_1,l_2)} \left[(1-\tau_0 p)^N + (1-(1-\tau_0)p)^N\right]$$

$$\cdot f_{\mathbf{L}}(l, l_1, l_2) dl dl_1 dl_2 + (1-p)^N, \qquad (29)$$

where τ_0 is described in (13) and (12).

Particularly, for the topology-independent random blockage model, the outage probability in (29) is given by:

$$\mathbb{P}_{\text{out}}^{(1\_\text{relay})}(p) = g_{p,3}^N(1) + g_{p,3}^N(2) - g_{p,3}^N(3), \tag{30}$$

where the function $g_{p,M}^N(k)$ is defined as

$$g_{p,M}^N(k) = 1 - \left(1 - k\frac{p}{M}\right)^N. \tag{31}$$

As the number of relays increases to 2, there are totally $M = \binom{2+2}{2} = 6$ links in the relay network. The outage probability with given blockage probability p and obstacle number N is

$$\mathbb{P}_{\text{out}}^{(2\_\text{relays})}(p) = g_{p,6}^N(1) + 2g_{p,6}^N(2) - 7g_{p,6}^N(4)$$
$$+ 7g_{p,6}^N(5) - 2g_{p,6}^N(6), \tag{32}$$

and the derivation of (32) is in Appendix B.

In the region with low blockage probability (for example, $p \leq 0.1$), by using the binomial theorem over (31) and omitting the higher order terms, we can approximate (30) and (32) by, respectively,

$$\mathbb{P}_{\text{out}}^{(1\_\text{relay})}(p) \approx 4\binom{N}{2}\left(\frac{p}{3}\right)^2, \tag{33}$$

and

$$\mathbb{P}_{\text{out}}^{(2\_\text{relay})}(p) \approx 12\binom{N}{3}\left(\frac{p}{6}\right)^3. \tag{34}$$

Similarly, given $m = 3$ or $m = 4$ relays as well as N obstacles, we can also derive the approximation of outage probability by following the method shown in Appendix B. With a similar approach in $m = 1, 2, 3$, and 4, $\mathbb{P}_{\text{out}}^{(m-\text{relays})}(p)$ for small p and general m in the topology-independent model can be expressed as

$$\mathbb{P}_{\text{out}}^{(m\_\text{relay})}(p) \approx 2(m+1)!\binom{N}{m+1}\left(\frac{p}{\binom{m+2}{2}}\right)^{m+1}. \tag{35}$$

However, the analysis becomes much more involved if the reflection is also exploited, and we will resort to the numerical evaluations for such situations.

IV. MAXIMUM THROUGHPUT PATH SELECTION

In this section we will develop an algorithm termed as *maximum throughput path selection* (MTPS) to find the path that maximizes the throughput for each source-destination pair. We denote the topology of the network by a graph $\mathcal{G} = (\mathcal{N}, \mathcal{A})$, where $\mathcal{N}$ is the set of all nodes in the network and $\mathcal{A}$ is the set of undirected connections between any pair of nodes. let $\mathcal{N}_r = \{1, 2, \ldots, |\mathcal{N}_r|\}$ be the set of relay nodes and let $\mathcal{N}_u$ be the set of user nodes, we have $\mathcal{N} = \mathcal{N}_r \cup \mathcal{N}_u$.

As discussed in Section II-A, a central coordinator is installed to manage and schedule the communications. It collects and updates user nodes' location information, monitors the status of blockage for user-relay links and relay-relay links, determines and executes path selections based on communications request, and coordinates concurrent communication tasks within the network. Since some parameters, such as

the dimension of the indoor space, dielectric constants ω of the reflection materials (walls, ceiling, floor), the position of deployed relaying nodes, and the antenna gains G_t and G_r, can be obtained at the installment and updated when necessary, we will assume that they are known at no extra cost. The path loss exponent n, the transmit power budget P_t at each individual node, and the background noise N_0 are long-term parameters and therefore can be updated with negligible overhead.

However, short-term parameters such as user nodes' current positions, the availability of the LOS links for user-relay and relay-relay paths, and the status of direct communications between any two nodes have to be updated at the central coordinator periodically to enable the proposed scheme. To ensure that the control signaling between the central coordinator and all other nodes can be delivered successfully, we assume that the central coordinator works in the omni- or quasi-omni mode and the control signaling channels are orthogonal to data transmission channels. Such orthogonal control channels can be established by dedicated time slots or system bandwidth. For instance, a time-division-duplex (TDD) based control plane is adopted in the WiGig specifications [1]. The allocation of dedicated control channels can be justified as follows. When the load of the system is not high, there are sufficient resources for both data transmission and control signaling; when the load is high, it is crucial to have orthogonal control signaling to minimize the possibility of collision, which could otherwise cause severe system performance degradation. The associated overhead will be analyzed in Section IV-C.

The proposed path selection can be done in three steps:

1) The coordinator monitors the network and updates a modified adjacency matrix following Algorithm 1;
2) Upon the request from a source-destination pair, the coordinator selects the path according to Algorithm 2;
3) The coordinator sends the communication schedule to the source-destination pair and the selected relay nodes.

Note that although our Algorithms 1 and 2 only focus on a single source-destination pair, multiple source-destination pairs can be scheduled concurrently by using orthogonal channels (e.g., in different time/frequency/beam). We will not elaborate on this as it is not the focus of this work.

A. Algorithm Description

The modified adjacency matrix $\mathbf{D} = [d_{uv}]$ indicates the effective distance between all pairs of nodes by taking into account link blockage and reflection. We first use a distance matrix $\tilde{\mathbf{D}}$ to denote the physical distance between any pair of nodes. That is, the entry $\tilde{d}_{uv}$ of $\tilde{\mathbf{D}}$ means the distance between the nodes u and v. Based on the status of the link, the adjacency matrix $\mathbf{D} = [d_{uv}]$ is updated by taking $d_{uv} = \tilde{d}_{uv} \cdot b_{uv}$, where $b_{uv} = 1$ means the existence of the LOS link, and $b_{uv} = \infty$ for the scenario with link blockage but no reflection, and $b_{uv} = \sqrt[n]{\chi(d_{uv})}$ for the scenario where the reflection path is available in the event of link blockage. The link status matrix $\mathbf{B} = [b_{uv}]$ is determined and updated based on the feedback from the relay and user nodes. The process of calculating the effective distance is shown in Algorithm 1.

Algorithm 1: Weighted Distance Calculation

Data: system location parameters, ω, and n

Input: distance matrix $\hat{\mathbf{D}} = \left[\hat{d}_{uv}\right]$

1 **if** *the reflection participates* **then**
2 | ReflectionOption $\leftarrow$ True;
3 **else**
4 | ReflectionOption $\leftarrow$ False;
5 **end**
6 **foreach** $(u, v) \in \mathcal{A}$ **do**
7 | **if** (u, v) *is blocked* **then**
8 | | **if** ReflectionOption = True **then**
9 | | | $b_{uv} \leftarrow \sqrt[n]{\chi(d_{uv})}$;
10 | | **else**
11 | | | $b_{uv} \leftarrow \infty$;
12 | | **end**
13 | **else**
14 | | $b_{uv} \leftarrow 1$;
15 | **end**
16 **end**
17 *Hadamard product*: $\mathbf{D} \leftarrow \tilde{\mathbf{D}} \circ \mathbf{B}$;

Output: modified adjacency matrix $\mathbf{D} = [d_{uv}]$

Note that although the size of the modified adjacency matrix $\mathbf{D}$ is $|\mathcal{N}| \times |\mathcal{N}|$, which can be large when there are many user nodes, only a few elements need to be updated regularly. First of all, $\mathbf{D}$ is symmetric, with a small sub-matrix of size $|\mathcal{N}_r| \times |\mathcal{N}_r|$ that is crucial for all kinds of communication requests. Secondly, for each new user node added into the system, we only need to add a new vector of length $|\mathcal{N}_r|$ to monitor the links between the new user node and all the relay nodes. Last but not the least, the links among all user nodes are only updated based on their updated position information and the corresponding link status parameters b_{uv} are not updated unless $\{u, v\}$ form a source-destination pair.

With the updated modified adjacency matrix $\mathbf{D}$, we find a path with the maximum throughput based on the MTPS procedure presented in Algorithm 2. We focus on a single source-destination pair $\{s, t\}$ and take $\mathcal{N} = \mathcal{N}_r \cup \{s, t\}$ to simplify the notation in the algorithm. In the algorithm, the sorted set $\mathcal{U}$ is used to denote the set of unselected relays, which is initialized by $\mathcal{N}_r$, and the entry $\mathcal{U}^{(i)}$, ($i \in \{1, 2, \ldots, |\mathcal{U}|\}$), represents the ith entry of $\mathcal{U}$. We use an indicator matrix $\mathcal{F} = [f_{ij}]$ to indicate that whether the rate of a link can be improved by using a relaying node. We use $\mathcal{P}$ to denote the current optimal path. The main steps of Algorithm 2 can be outlined as follows:

1) Initialize $\mathcal{P} = \{(s, t)\}$, $\mathcal{U} = \mathcal{N}_r$, and $\mathbf{D} = \mathbf{0}$;
2) For each hop $i \rightarrow j$ of the current path $\mathcal{P}$, if it is not locked ($f_{ij} = 0$) and at least one relay from $\mathcal{U}$ is in the relay-prioritized region, we find the relay node $r \in \mathcal{U}$ with the highest throughput, and remove it from $\mathcal{U}$, and split the original hop $i \rightarrow j$ two new hops $i \rightarrow r$ and $r \rightarrow j$.
3) Update the current optimal path;
4) If the updated path remains the same as the previous one, output the current path and exit; otherwise, go back to 2).

B. Maximum Throughput Calculation

Assuming that there are L hops for a path with half-duplex relays, and the rate over the i-th hop is denoted by R_i, where $i \in \{1, 2, \ldots, L\}$, then the throughput of the L-hop relay path is given by Proposition 4.

Algorithm 2: Maximum Throughput Path Selection

Data:
- effective distance $\mathbf{D} = [d_{uv}]$;
- aggregated parameter α and path loss exponent n;

Input:
- initial path set $\mathcal{P} = \{(s, t)\}$;
- unselected relays set $\mathcal{U} = \mathcal{N}_r$;

1 Initialize the link-lock matrix $\mathbf{F} = [f_{uv}] = \mathbf{0}_{|\mathcal{N}_r| \times |\mathcal{N}_r|}$;
2 Calculate critical distance $l^* \leftarrow \sqrt[n]{\frac{\alpha}{2^n - 2}}$;
3 Set termination condition TerminateFlag $\leftarrow$ False;
4 **while** TerminateFlag = False **do**
5 | $\mathcal{P}' \leftarrow \emptyset$;
6 | **foreach** $(i, j) \in \mathcal{P}$ **do**
7 | | SubstituteFlag $\leftarrow$ False;
8 | | $\mathcal{P}^* \leftarrow \{(i, j)\}$;
9 | | **if** $d_{ij} \geq l^*$ **and** $f_{ij} = 0$ **then**
10 | | | $R_{\max} \leftarrow R(d_{ij})$;
11 | | | **for** $k \leftarrow 1$ **to** $|\mathcal{U}|$ **do**
12 | | | | $r \leftarrow \mathcal{U}^{(k)}$;
13 | | | | $R_{\max}^* \leftarrow \rho(R(d_{ir}), R(d_{rj}))$;
14 | | | | **if** $R_{\max}^* \geq R_{\max}$ **then**
15 | | | | | $R_{\max} \leftarrow R_{\max}^*$;
16 | | | | | $\mathcal{P}^* \leftarrow \{(i, r), (r, j)\}$;
17 | | | | | $r^* \leftarrow r$;
18 | | | | | SubstituteFlag $\leftarrow$ True;
19 | | | **end**
20 | | **end**
21 | | **if** SubstituteFlag = True **then**
22 | | | $\mathcal{U} \leftarrow \mathcal{U} - \{r^*\}$;
23 | | **else**
24 | | | $f_{ij} \leftarrow 1$;
25 | | **end**
26 | | **else**
27 | | | $f_{ij} \leftarrow 1$;
28 | | **end**
29 | | $\mathcal{P}' \leftarrow \mathcal{P}' \cup \mathcal{P}^*$;
30 | **end**
31 | **if** $\mathcal{P}' = \mathcal{P}$ **then**
32 | | $\mathcal{P}_{opt} \leftarrow \mathcal{P}$;
33 | | TerminateFlag $\leftarrow$ True;
34 | **else**
35 | | $\mathcal{P} \leftarrow \mathcal{P}'$;
36 | **end**
37 **end**

Output: the optimal path set $\mathcal{P}_{opt}$

Proposition 4: For an L-hop channel, let R_i be the capacity of each individual channel i, $i = 1, 2, \ldots, L$, the maximum achievable rate R^* over the cascaded channel under the half-duplex constraint is given by:

$$R^* = \min\left\{\frac{R_1 R_2}{R_1 + R_2}, \frac{R_2 R_3}{R_2 + R_3}, \cdots, \frac{R_{L-1} R_L}{R_{L-1} + R_L}\right\}. \quad (36)$$

Proof: For an L-hop network consisting of $L - 1$ half-duplex relaying nodes, we assume each relaying node k, $k \in \{1, 2, \ldots, L - 1\}$, connecting the kth and $(k+1)^{\text{th}}$ hop, has a transmitting state, a receiving state and a silent state with corresponding durations ξ_k^{t}, ξ_k^{r}, and ξ_k^{s}, respectively. We have a duration constraint as follows:

$$\xi_k^{\text{t}} + \xi_k^{\text{r}} + \xi_k^{\text{s}} = 1, \quad k \in \{1, 2, \ldots, L - 1\}. \quad (37)$$

Clearly, the end-to-end throughput is the maximum achievable flow through all intermediate nodes. We assume that a packet of size R goes through each node within a unit duration. At relaying node k, the durations of receiving and transmitting states are respectively given by:

$$\xi_k^{\mathrm{r}} = \frac{R}{R_k}, \quad \xi_k^{\mathrm{t}} = \frac{R}{R_{k+1}}, \tag{38}$$

where R_{k-1} and R_k are the channel capacities of kth and $(k+1)^{\text{th}}$ hop, respectively. Combining with the constraint in (37), we have the silence duration as the function of R:

$$\xi_k^{\mathrm{s}}(R) = 1 - \frac{R_k + R_{k+1}}{R_k R_{k+1}} R = 1 - s_k R. \tag{39}$$

Thus, for all $k \in \{1, 2, \ldots, L-1\}$, we can obtain a cluster of linear functions $\xi_k^{\mathrm{s}}(R)$. We find that $\xi_k^{\mathrm{s}}(R)$ decays by increasing R with the slope $-s_k$. In addition, by considering the fact that for each relaying node k, we always have $\xi_k^{\mathrm{s}}(R) \geq 0$, the problem can be reformulated as:

$$
\begin{aligned}
R^* &= \max_{\substack{\xi_k^{\mathrm{s}}(R) \geq 0 \\ k \in \{1,2,\ldots,L-1\}}} R \\
&= \min_{k \in \{1,2,\ldots,L-1\}} \frac{1}{s_k} = \min_{k \in \{1,2,\ldots,L-1\}} \frac{R_k R_{k+1}}{R_k + R_{k+1}}.
\end{aligned} \tag{40}
$$

Therefore, within a time slot, a packet with the size at most R^* can be transmitted from the source to the sink. This concludes the maximum achievable rate shown in (36). $\square$

Note that the maximum throughput provided by Proposition 4 holds only if the amount of transmitted data goes to infinity. As a simple example, we assume there is one optimal routing path $\mathcal{P}$ between the source and destination, consisting of L hops with the maximum transmission rate R in each hop. By following (36), we obtain the theoretically maximum throughput $R^* = R/2$. Now we assume K packets, each size of R_p, are to be transmitted. Thus the effective rate over the path is given by:

$$R_{\mathrm{eff}} = \frac{KR_p}{\frac{R_p}{R}L + \frac{R_p}{R}(2K-1)} = \frac{KR}{2K + L - 1} \leq R^*. \tag{41}$$

It is clear that for finite K, the effective rate is strictly smaller than the theoretical optimal results given by Proposition 4. Yet for a large K, R_{eff} shall approach R^*. Hence, here we assume K is large enough such that

$$\frac{L-1}{K} \to 0 \Longrightarrow R_{\mathrm{eff}} \to R^*. \tag{42}$$

C. Complexity Analysis

The computational complexity of the MTPS algorithm consists of two parts: calculating the throughput of paths and comparing the throughput. From (40), the complexity of the throughput calculation can be measured by the number of the $\min(\cdot, \cdot)$ operation, which outputs the smaller value of two arguments. It is evident that if we want to find the minimum of q inputs, the $\min(\cdot, \cdot)$ operator will be recursively applied $q - 1$ times. For comparing the throughput, the complexity for finding

the optimal path is evaluated by the number of the $\max(\cdot, \cdot)$ operation, which outputs the larger input.

For the brute-force algorithm with exhaustive search, given n relays, there are $k!\binom{n}{k}$ distinct paths of $k+1$, $(k = 0, 1, \ldots, n)$ hops connecting the transmitter and the receiver. To calculate the throughput of an i-hop path, $i - 1$ $\min(\cdot, \cdot)$ operations are needed. Thus the complexity is given by $\sum_{k=0}^{n} k \cdot k!\binom{n}{k}$. To find the paths with the maximum throughput, $\sum_{k=0}^{n} k!\binom{n}{k}$ comparisons are needed since there are $\sum_{k=0}^{n} k!\binom{n}{k}$ different paths. Let $T_1(n)$ denote the number of $\min(\cdot, \cdot)$ or $\max(\cdot, \cdot)$ operations for the network with n relays, we have

$$T_1(n) = \sum_{k=0}^{n} \frac{k \cdot n!}{(n-k)!} + \sum_{k=0}^{n} \frac{n!}{(n-k)!} - 1 \in \mathcal{O}(n \cdot n!), \tag{43}$$

since

$$\lim_{n \to \infty} \frac{T_1(n)}{n \cdot n!} = \lim_{n \to \infty} \left(\frac{1}{n} \sum_{k=0}^{n} \frac{k+1}{(n-k)!} - \frac{1}{n \cdot n!} \right) = e, \tag{44}$$

where $e = 2.718\cdots$ is the Euler's number.

Similarly, we define $T_2(n)$ the number of $\min(\cdot, \cdot)$ or $\max(\cdot, \cdot)$ operations for the MTPS algorithm. For the worst case, only one available relay is selected within each iteration to replace one hop, and other hops will be locked for the path. In such scenario, within each iteration, the number of $\min(\cdot, \cdot)$ equals to that of $\max(\cdot, \cdot)$. This is because each hop will be replaced by possible 2-hops, which need comparison operations subsequently. Thus, the complexity of the MTPS algorithm is given by:

$$T_2(n) = 2 \left(n + 2 \sum_{k=1}^{n-1} (n-k) \right) = 2n^2 \in \mathcal{O}(n^2). \tag{45}$$

Comparing (43) and (45), we see that the MTPS algorithm can significantly reduce the complexity compared to the brute-forced algorithm when the number of relays are large.

The signaling overhead of the protocol is small. On one hand, the amount of data that needs to periodically updated is small. For example, the availability of the LOS paths for user-relay or relay-relay links and the status of any direct user-user transmission only account for a few bits from each node (a few bits for link identity and another bit for LOS availability). The positioning information is at most 30 bytes [36], [37]. Given the fact that the data transmission rate is in the order of 100 Mbps, the time needed for transmitting control signaling for each user node is around 10 microseconds.[3] The readers are also referred to [32] for an estimate with similar results. On the other hand, the periodicity of the parameter update is relatively large since the mobility of users/obstacles is very slow in the indoor environment. For example, given a beamwidth of $12°$ and communication distance of 5 meters, it takes roughly 500 milliseconds for the node to move from the center of the beam to its edge and thus invalidate the previous position information, if the velocity is 1 meter per second. Combining the above two factors, and given the fact that there cannot be

---

[3]Here we also take into account the rate degradation caused by using omnidirectional antenna pattern at the central coordinator for control signaling.

TABLE III
SIMULATION PARAMETERS

Parameters	Symbol	Value
Bandwidth	W	1200 MHz
Transmitting Power	P_t	0.1 mW
Transmitter Antenna Gain	G_t	15 dB
Receiver Antenna Gain	G_r	15 dB
Path Loss Exponent	n	3
Background Noise	N_0	-114 dBm/MHz
Wavelength	λ	5×10^{-3} m
Dielectric Constant of Ceiling	ω	$6.14 - j0.3015$
Distance to Reflective Ceiling	h	3 m
Number of Obstacles	N	20
Radius of Relay Placement	r	3 m
Radius of Circular Hall	R_0	15 m

Fig. 3. Average throughput [Mbps] versus link blockage probability p for topology-independent models, where $N = 20$ obstacles are randomly distributed within a circular hall of radius $R_0 = 15$ meters and the half-duplex relay node is deployed at the center of the hall. The default transmit power is $P_t = 0.1$ mW with bandwidth $W = 1200$ MHz.

too many users in indoor environment (say maximum 1 user per square meter), the aggregate overhead of the control signaling is less than 1%.

V. PERFORMANCE EVALUATION

In this section, we present simulation results on average throughput and outage performance for both topology-dependent and topology-independent blockage models with different numbers of relay nodes deployed inside a circular hall of radius $R_0 = 15$ meters, where $N = 20$ obstacles are randomly distributed with link blockage probability $p \in [0, 1]$. To simplify simulation, we assume that all the nodes are placed on the same horizontal plane above the ground, and the ceiling of the indoor environment is supposed to be always available for wave reflection. The distance between the transmitter-receiver plane and the reflection ceiling is defined as h, and the common simulation parameters are summarized in Table III, which corresponds to the SNR of 35 dB at 1-meter LOS transmission distance and 5 dB at 10-meter distance.

Furthermore, we assume that all the antennas are situated at the same horizontal plane as defined by the height of the nodes, which will allow us to characterize the radiation pattern in a 2-D fashion.[4] Given azimuthal angle coordinate ϕ and beamwidth Δ_b, the antenna gain can be determined by using the idealized *flat-top model* [38] as follows,

$$G(\phi) = \begin{cases} \frac{2\pi}{\Delta_b}, & |\phi| \leq \frac{\Delta_b}{2} \\ 0, & \text{otherwise.} \end{cases} \quad (46)$$

With the antenna gain of 15 dB given by Table III, we have the beamwidth $\Delta_b = 11.4°$.

A. Average Throughput

We first evaluate the average throughput for four communications scenarios, namely, LOS, (LOS, Relay), (LOS, Reflection), and (LOS, Relay, Reflection). We increase the link blockage
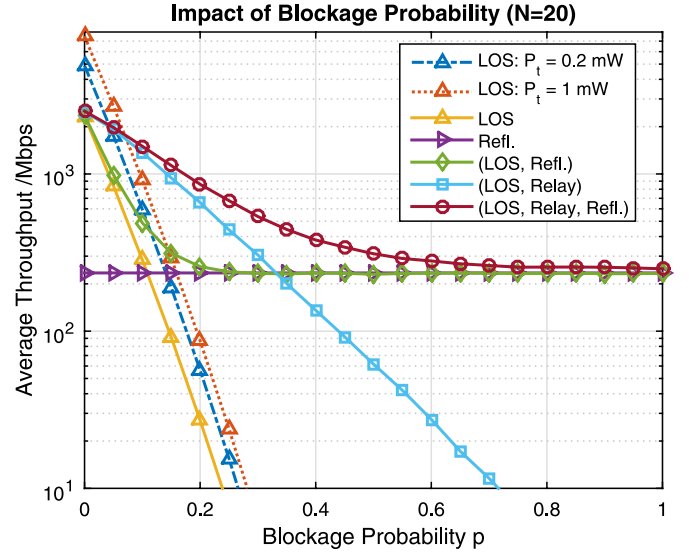
probability from 0 to 1 to demonstrate the benefits of resorting to relaying and/or reflection, the dependence of the two random blockage models, and the influence of the number of deployed relaying nodes.

1) One Relay Scenario: In Fig. 3 we demonstrate the benefits of resorting to relaying and/or reflection under the topology-independent random blockage model. We can see that, when there are many obstacles (N = 20) with link blockage probability $p \in (0.1, 0.2)$, the average throughput can be increased by approximately 10 times by introducing a half-duplex relay node. The benefit of resorting to reflection paths, which is not significant for small p (< 0.05), outweighs that of relaying for $p > 0.35$. Note that, without reflection, the average throughput for the LOS and (LOS, relay) scenarios both decreases dramatically, but adding a relay node can significantly slow down the performance degradation trend. When reflection is taken into account, average throughput of roughly 290 Mbps is still available even for very high link blockage probability, which is well in line with our analysis in (23). Therefore, resorting to reflection is capable to provide the minimum guarantee on average throughput when the other transmission paths are unavailable. We also plot two curves for LOS scenarios with increased transmit power $P_t = 0.2$ mW (dashed line, 3 dB power gain) and $P_t = 1$ mW (dotted line, 10 dB power gain), respectively. Although increasing the transmit power can improve the average throughput, it is not an effective way to combat link blockage.

In Fig. 4 we evaluate the influence of blockage modeling on the performance of average throughput. For the (LOS, Relay) scenario, the difference between the average throughput of two blockage models can be huge, especially when the blockage probability p is large. The gap is much smaller when reflection is also taken into consideration since the reflection paths are assumed to be always available (say via ceiling) and therefore not subject to link blockage.

---

[4]Usually, directional antennas are characterized by the radiation pattern in the 3-D fashion, which relates to the elevation and azimuth beamwidth.
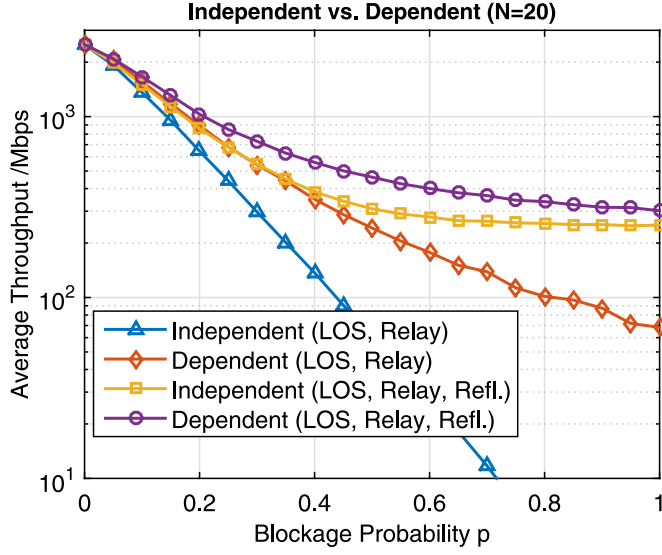
Fig. 4. Impact of blockage probability p on average throughput [Mbps] in the topology-dependent or topology-independent model, where the (LOS, Relay) and (LOS, Relay, Reflection) scenarios are employed.
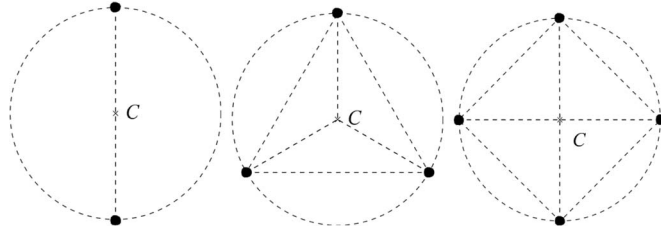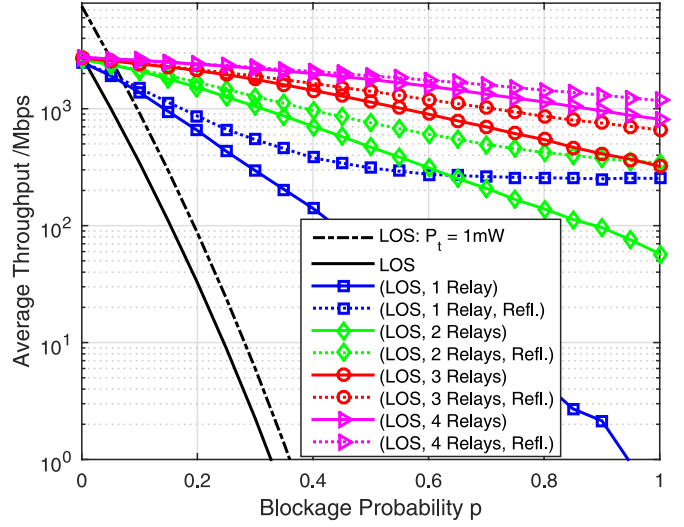

Fig. 6. Average throughput performance for the multi-relay scenarios with blockage in topology-independent model, where the relays are following the deployment shown in Fig. 5.
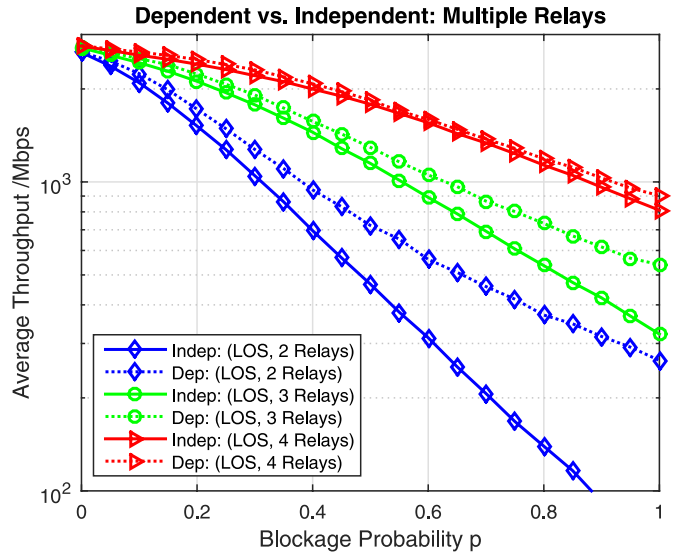

Fig. 5. The placement patterns for multiple relays that are uniformly scattered on the circle with the radius $r = 3$ m in the room with radius $R_0 = 15$ m.

2) Multi-Relay Scenarios: In Fig. 6 we evaluate the benefit of deploying multiple relaying nodes under the topology-independent model, where 2 to 4 relays are uniformly distributed on the circle with the radius $r = 3$ meters according to the placement patterns shown in Fig. 5. As the number of relaying nodes increases, the average throughput is improved significantly for almost all range of link blockage probability ($p > 0.05$). At $p = 0$, the improvement of increasing the number of relays is almost invisible since the probability of increasing the rate by using a half-duplex relaying node is small given the relatively small radius of the hall ($R_0 = 15$ meters). Another interesting observation in Fig. 6 is that average throughput guarantee can also be realized by increasing the number of deployed relaying nodes, and the importance of reflection paths is no longer remarkable even when p is large.

On the other hand, Fig. 7 shows that the strong influence of blockage modeling still remains for multi-relay scenarios, very similar to what we have observed in Fig. 4. Besides, a more interesting phenomenon will happen if we have higher antenna gains, that is, the topology-dependent model will be surpassed by its topology-independent counterpart in terms of average throughput when the number of relays is increased to a certain value, which also implies the influence of blockage modeling. Here, we are not going to provide those simulations due to the space limitation.

Fig. 7. Average throughput [Mbps] for (LOS, relay) with multiple relaying nodes under topology-dependent or topology-independent models.

B. Outage Probability

We first investigate the influence of blockage modelling on the availability of LOS and relay links. In Fig. 8 we plot the event probabilities $\mathbb{P}\{E_i\}$, $i \in \{1, 2, 3, 4\}$, indicating the availability of the LOS and/or the relay paths for the (LOS, Relay) scenario, where

$$\mathbb{P}\{E_i\} = \iiint\limits_{(l,l_1,l_2)} \mathbb{P}\{E_i|\mathbf{L}\} f_{\mathbf{L}}(l, l_1, l_2) dl dl_1 dl_2, \quad (47)$$

and $\mathbb{P}\{E_i\}$, $i = 1, 2, 3, 4$, corresponding to the four blockage situations of (LOS, Relay) scenario, are presented in (17), (18), (19), and (20), respectively. We observe that, except for E_1, the probability for two blockage models differs significantly for some range of p. If we maintain connectivity by choosing
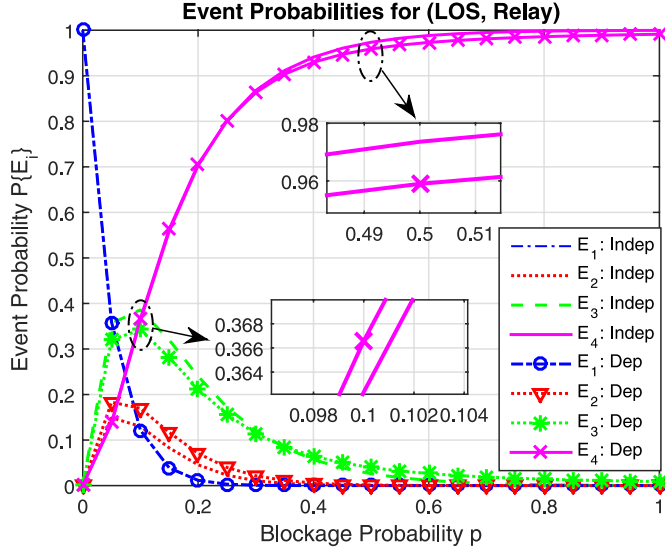
Fig. 8. The event probabilities $\mathbb{P}\{E_i\}$, $i = 1, 2, 3, 4$, for the (LOS, Relay) scenario regarding the availability of the LOS and/or the relaying paths under topology-dependent or topology-independent models. $\mathbb{P}\{E_i\}$, $i = 1, 2, 3, 4$, correspond to four blockage situations presented in (17), (18), (19), and (20), respectively.
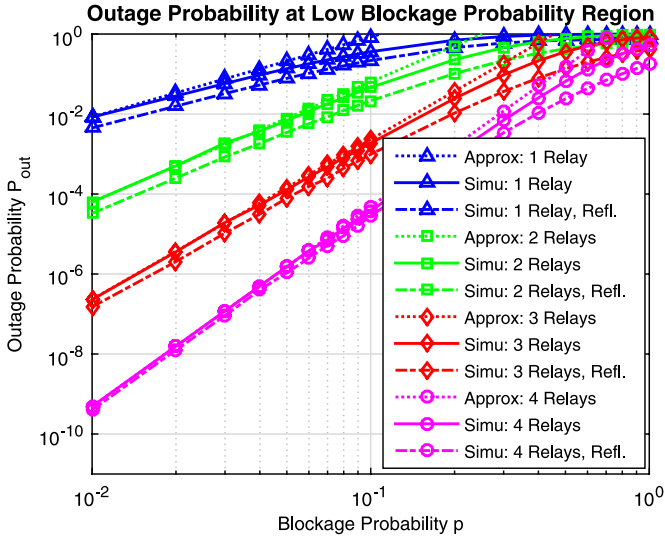

Fig. 9. Outage probability for scenarios with different number of relays under the topology-independent model where the threshold rate is set to $R_\epsilon = 605$ Mbps. The approximated and simulated outage performances are also provided.

a lower threshold, the outage probability $\mathbb{P}_{\text{out}}^{(1\_\text{relay})}(p) = \mathbb{P}\{E_4\}$ is shown in (29). From numerical evaluations we can see that the topology-dependent model has higher $\mathbb{P}\{E_4\}$ than that of the topology-independent model for $p \leq 0.23$ and smaller otherwise (as shown in the zoom-in details), which implies that the comparison of the two random blockage models should be related to the underlining link blockage probability, which coincides with what we conclude from Fig. 7.

In Fig. 9 we investigate the outage performance under the topology-independent random blockage model where the rate threshold is set to $R_\epsilon = R(2R_0) = 605$ Mbps. When p is small, the approximated outage probability given by (35) matches

well with the simulation results. It also shows that the outage probability can be remarkably reduced by increasing the number of relays. Resorting to the reflection paths, however, can only provide marginal contribution for low blockage probability cases. This is in line with what we have observed in the simulation results for average throughput.

VI. CONCLUSION

We have investigated the throughput and outage performance of indoor 60 GHz communications over relay networks, where the communication between two nodes can be established either by the LOS path, via a half-duplex relaying node, or via the reflection path. A central coordinator is deployed to collect the topology information of nodes and to manage the path selection and scheduling. We consider both topology-independent and topology-dependent random blockage models and analyze the performance of average throughput and outage probability. To increase the throughput for networks with multiple relays, we propose the MTPS algorithm to select the optimal transmission path. Given n relay nodes, we show that the complexity of the proposed algorithm is $\mathcal{O}(n^2)$, in contrast to $\mathcal{O}(n \cdot n!)$ by the brute-force approach. Simulation results show that increasing the number of relays can substantially increase the average throughput and decrease the outage probability. Reflection path, on the other hand, is very useful to keep the connectivity and lower the outage probability when the link blockage probability is high. Furthermore, we have observed that different blockage models can significantly affect the performance of average throughput and outage probability. Therefore, it is crucial to determine the suitable types of random blockage models when analyzing and evaluating different communications schemes for a specific network configuration.

In future, we will explore the influence of interference from concurrent transmission on the performance of the MTPS algorithm. Besides, it would be interesting and crucial to determine which model is more suitable to model the random blockage events in different indoor situations, and what's the impact of the probabilistic path loss model [39] on the design of optimal path selection algorithms.

APPENDIX A
PROOF OF PROPOSITION 1

We assume the propagation distance is much larger than the wavelength. We denote by E_{in} and E_{refl} the electric fields of incident and reflected waves at the reflection point, respectively. According to the *Fresnel Reflection Formula*, we have $E_{\text{refl}} = |\eta| E_{\text{in}}$, where η is given in (6). As shown in Fig. 2, the distance of the LOS path between two points $N_1(x_1, y_1)$ and $N_2(x_2, y_2)$ is $l = \sqrt{(x_1 - x_2)^2 + (y_1 - y_2)^2}$ and the distance of the reflection path is $l' = \sqrt{(x_1 - x_2)^2 + (y_1 + y_2)^2}$. The incident angle θ is determined as

$$\theta = \arctan \left| \frac{x_2 - x_1}{y_2 + y_1} \right|. \tag{48}$$
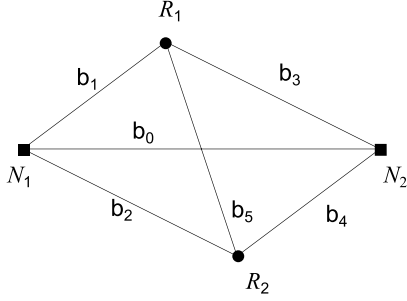
Fig. 10. The scenario with two relays, namely R_1 and R_2, where N_1 and N_2 are two wireless devices.

The path loss of the LOS path and the reflection path are therefore (measured in dB)

$$L_{N_1 N_2}(l) = 20 \log\left(\frac{4\pi}{\lambda}\right) + 10n \log(l), \tag{49}$$

$$L_{N_1' N_2}(l', \theta) = 20 \log\left(\frac{4\pi}{\lambda}\right) + 10n \log(l') - 20 \log|\eta(\theta)|. \tag{50}$$

Subtracting (49) from (50) provides (5).

In a special case with $y_1 = y_2 = h$, we have $l = |x_1 - x_2|$ and $l' = \sqrt{d^2 + 4h^2}$ and the incident angle θ can be obtained by $\theta = \arctan\left(\frac{d}{2h}\right)$. Once h is known and fixed, both l' and θ can be regarded as the functions of l and therefore $\chi(l, l', \theta)$ can be reduced to a function of only l for given h,

$$\chi(l) = 5n \log\left(1 + \frac{4h^2}{l^2}\right) - 20 \log\left|\frac{\sqrt{(\omega-1)l^2 + 4\omega h^2} - 2\omega h}{\sqrt{(\omega-1)l^2 + 4\omega h^2} + 2\omega h}\right|. \tag{51}$$

APPENDIX B
DERIVATION OF EQUATION (32)

As depicted in Fig. 10, N_1 and N_2 are the user terminals, and R_1 and R_2 represent two relays, respectively. The label b_k, $k \in \{0, 1, \ldots, 5\}$ on each arrow of the graph denotes the blockage event over the corresponding link. Clearly, there are four link blockage patterns X_i, $i = 1, 2, 3, 4$, to disconnect the communication between N_1 and N_2, where $X_1 = b_0 b_1 b_2$, $X_2 = b_0 b_3 b_4$, $X_3 = b_0 b_1 b_5 b_4$ and $X_4 = b_0 b_2 b_5 b_3$. The outage happens if any of the four link blockage patterns occurs. Thus, the outage probability is given by:

$$\mathbb{P}_{\text{out}}^{(2\_\text{relay})} = \mathbb{P}\{X_1 \cup X_2 \cup X_3 \cup X_4\}$$

$$= \sum_{i=1}^{4} \mathbb{P}\{X_i\} - \sum_{i<j} \mathbb{P}\{X_i X_j\} + \sum_{i<j<k} \mathbb{P}\{X_i X_j X_k\}$$

$$- \sum_{i<j<k<l} \mathbb{P}\{X_i X_j X_k X_l\}. \tag{52}$$

By expressing X_i, $i = 1, 2, 3, 4$ in b_k, $k \in \{0, 1, \ldots, 5\}$ and using the inclusion-exclusion principle iteratively, the outage probability can be obtained.
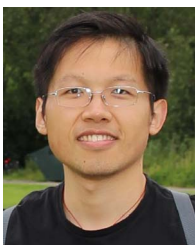
REFERENCES

[1] "Defining the future of multi-gigabit wireless communications," Wireless Gigabit Alliance, Austin, TX, USA, White Paper, 2010.

[2] N. Moraitis and P. Constantinou, "Indoor channel measurements and characterization at 60 GHz for wireless local area network applications," *IEEE Trans. Antennas Propag.*, vol. 52, no. 12, pp. 3180–3189, Dec. 2004.

[3] P. F. Smulders, "Statistical characterization of 60-GHz indoor radio channels," *IEEE Trans. Antennas Propag.*, vol. 57, no. 10, pp. 2820–2829, Oct. 2009.

[4] N. Moraitis and P. Constantinou, "Measurements and characterization of wideband indoor radio channel at 60 GHz," *IEEE Trans. Wireless Commun.*, vol. 5, no. 4, pp. 880–889, Apr. 2006.

[5] S. Geng, J. Kivinen, X. Zhao, and P. Vainikainen, "Millimeter-wave propagation channel characterization for short-range wireless communications," *IEEE Trans. Veh. Technol.*, vol. 58, no. 1, pp. 3–13, Jan. 2009.

[6] M. Williamson, G. Athanasiadou, and A. Nix, "Investigating the effects of antenna directivity on wireless indoor communication at 60 GHz," in *Proc. 8th IEEE Int. Symp. PIMRC*, 1997, pp. 635–639.

[7] R. C. Daniels and R. W. Heath, "60 GHz wireless communications: Emerging requirements and design recommendations," *IEEE Veh. Technol. Mag.*, vol. 2, no. 3, pp. 41–50, Sep. 2007.

[8] C. Park and T. S. Rappaport, "Short-range wireless communications for Next-Generation Networks: UWB, 60 GHz millimeter-wave WPAN, and ZigBee," *IEEE Wireless Commun.*, vol. 14, no. 4, pp. 70–78, Aug. 2007.

[9] N. Guo, R. C. Qiu, S. S. Mo, and K. Takahashi, "60-GHz millimeter-wave radio: Principle, technology, and new results," *EURASIP J. Wireless Commun. Netw.*, vol. 2007, no. 1, pp. 48–48, Jan. 2007.

[10] M. Jacob *et al.*, "A ray tracing based stochastic human blockage model for the IEEE 802.11 ad 60 GHz channel model," in *Proc. 5th EUCAP*, 2011, pp. 3084–3088.

[11] C. Gustafson and F. Tufvesson, "Characterization of 60 GHz shadowing by human bodies and simple phantoms," in *Proc. 6th EUCAP*, 2012, pp. 473–477.

[12] S. Collonge, G. Zaharia, and G. E. Zein, "Influence of the human activity on wide-band characteristics of the 60 GHz indoor radio channel," *IEEE Trans. Wireless Commun.*, vol. 3, no. 6, pp. 2396–2406, Nov. 2004.

[13] M. Jacob *et al.*, "Fundamental analyses of 60 GHz human blockage," in *Proc. 7th EUCAP*, 2013, pp. 117–121.

[14] A. Maltsev *et al.*, *Channel models for 60 GHz WLAN systems*, IEEE P802.11 Wireless LANs, May 2010.

[15] K. Dong, X. Liao, and S. Zhu, "Link blockage analysis for indoor 60 GHz radio systems," *Electron. Lett.*, vol. 48, no. 23, pp. 1506–1508, Nov. 2012.

[16] S. Singh, F. Ziliotto, U. Madhow, E. Belding, and M. Rodwell, "Blockage and directivity in 60 GHz wireless personal area networks: From cross-layer model to multihop MAC design," *IEEE J. Sel. Areas Commun.*, vol. 27, no. 8, pp. 1400–1413, Oct. 2009.

[17] C. S. Leong, B. S. Lee, A. R. Nix, and P. Strauch, "A robust 60 GHz wireless network with parallel relaying," in *Proc. IEEE ICC*, 2004, pp. 3528–3532.

[18] Z. Genc, G. M. Olçer, E. Onur, and I. Niemegeers, "Improving 60 GHz indoor connectivity with relaying," in *Proc. IEEE ICC*, 2010, pp. 1–6.

[19] Z. Lin, X. Peng, F. Chin, and W. Feng, "Outage performance of relaying with directional antennas in the presence of co-channel interferences at relays," *IEEE Wireless Commun. Lett.*, vol. 1, no. 4, pp. 288–291, Aug. 2012.

[20] Z. Genc, U. H. Rizvi, E. Onur, and I. Niemegeers, "Robust 60 GHz indoor connectivity: Is it possible with reflections?" in *Proc. IEEE 71st VTC—Spring*, 2010, pp. 1–5.

[21] X. An *et al.*, "Beam switching support to resolve link-blockage problem in 60 GHz WPANs," in *Proc. IEEE 20th Int. Symp. Pers., Indoor Mobile Radio Commun.*, 2009, pp. 390–394.

[22] S. Sun, T. S. Rappaport, R. Heath, A. Nix, and S. Rangan, "Mimo for millimeter-wave wireless communications: Beamforming, spatial multiplexing, or both?" *IEEE Commun. Mag.*, vol. 52, no. 12, pp. 110–121, Dec. 2014.

[23] L. Cai, H. Hwang, X. Shen, J. Mark, and L. Cai, "Optimizing geographic routing for millimeter-wave wireless networks with directional antenna," in *Proc. 6th Int. Conf. BROADNETS*, 2009, pp. 1–8.

[24] H. Su and X. Zhang, "Joint link scheduling and routing for directional-antenna based 60 GHz wireless mesh networks," in *Proc. IEEE GLOBECOM*, 2009, pp. 1–6.

[25] Z. Lan *et al.*, "Relay with deflection routing for effective throughput improvement in Gbps millimeter-wave WPAN systems," *IEEE J. Sel. Areas Commun.*, vol. 27, no. 8, pp. 1453–1465, Oct. 2009.

[26] C.-F. Shih, W. Liao, and H.-L. Chao, "Joint routing and spectrum allocation for multi-hop cognitive radio networks with route robustness consideration," *IEEE Trans. Wireless Commun.*, vol. 10, no. 9, pp. 2940–2949, Sep. 2011.

[27] Z. Fan, "Wireless networking with directional antennas for 60 GHz systems," in *Proc. 14th EW Conf.*, 2008, pp. 1–7.

[28] L. X. Cai, L. Cai, X. Shen, and J. W. Mark, "REX: A randomized exclusive region based scheduling scheme for mmWave WPANs with directional antenna," *IEEE Trans. Wireless Commun.*, vol. 9, no. 1, pp. 113–121, Jan. 2010.

[29] J. Qiao, L. X. Cai, X. Shen, and J. W. Mark, "Enabling multi-hop concurrent transmissions in 60 GHz wireless personal area networks," *IEEE Trans. Wireless Commun.*, vol. 10, no. 11, pp. 3824–3833, Nov. 2011.

[30] J. Park and C. Nguyen, "A new millimeter-wave step-frequency radar sensor for distance measurement," *IEEE Microw. Wireless Compon. Lett.*, vol. 12, no. 6, pp. 221–222, Jun. 2002.

[31] K. Haddadi, M. Wang, D. Glay, and T. Lasri, "A 60 GHz six-port distance measurement system with sub-millimeter accuracy," *IEEE Microw. Wireless Compon. Lett.*, vol. 19, no. 10, pp. 644–646, Oct. 2009.

[32] *Millimeter-Wave-Based Alternative Physical Layer Extension*, IEEE Std. 802.15.3c-2009 (Amendment to IEEE Std 802.15.3-2003), 2009.

[33] D. Barton, F. David, and E. Fix, "Random points in a circle and the analysis of chromosome patterns," *Biometrika*, vol. 50, no. 1/2, pp. 23–29, Jun. 1963.

[34] J. Deissner, J. Hubner, D. Hunold, and J. Voigt, RPS Radiowave Propagation Simulator User Manual Version 5.4, 2008.

[35] R. Azzam, "Relationship between the p and s Fresnel reflection coefficients of an interface independent of angle of incidence," *J. Opt. Soc. Amer. A, Opt. Image Sci.*, vol. 3, no. 7, pp. 928–929, Jul. 1986.

[36] M. Cypriani, F. Lassabe, P. Canalda, and F. Spies, "Open wireless positioning system: A Wi-Fi-based indoor positioning system," in *Proc. IEEE 70th VTC—Fall*, 2009, pp. 1–5.

[37] H. Liu, H. Darabi, P. Banerjee, and J. Liu, "Survey of wireless indoor positioning techniques and systems," *IEEE Trans. Syst., Man, Cybern., C, Appl. Rev.*, vol. 37, no. 6, pp. 1067–1080, Nov. 2007.

[38] J. E. Wieselthier, G. D. Nguyen, G. D, and A. Ephremides, "Energy-aware wireless networking with directional antennas: The case of session-based broadcasting and multicasting," *IEEE Trans. Mobile Comput.*, vol. 1, no. 3, pp. 176–191, Jul.–Sep. 2002.

[39] M. Samimi, T. Rappaport, and G. MacCartney, "Probabilistic omnidirectional path loss models for millimeter-wave outdoor communications," *IEEE Wireless Commun. Lett.*, to be published.
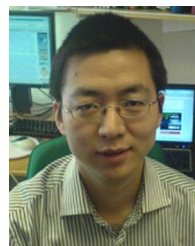
Jinfeng Du (S'07–M'13) received the B.Eng. degree in electronic information engineering from the University of Science and Technology of China (USTC), Hefei, China, in 2004, and the M.Sc. degree in electronic engineering, Tekn. Lic. degree in electronics and computer systems, and Ph.D. degree in telecommunications, all from the Royal Institute of Technology (KTH), Stockholm, Sweden, in 2006, 2008, and 2012, respectively. He is currently a Postdoctoral Researcher in the Research Laboratory of Electronics, Massachusetts Institute of Technology, Cambridge, MA, USA.

Dr. Du received the Best Paper Award from IC-WCSP in October 2010 and his paper was elected as one of the "Best 50 Papers" at IEEE GLOBECOM 2014. He received the prestigious Hans Werthén Grant from the Royal Swedish Academy of Engineering Science (IVA) in 2011, the Chinese Government Award for Outstanding Self-Financed Students Abroad in 2012, and the International PostDoc grant from the Swedish Research Council in 2013. He also received three grants from the Ericsson Research Foundation in 2011, 2013, and 2015.

Ming Xiao (S'02–M'07–SM'12) received the bachelor and master degrees in engineering from the University of Electronic Science and Technology of China, Chengdu, China, in 1997 and 2002, respectively, and the Ph.D. degree from Chalmers University of Technology, Göteborg, Sweden, in November 2007. From 1997 to 1999, he worked as a Network and Software Engineer at ChinaTelecom. From 2000 to 2002, he also held a position in the SiChuan communications administration. Since November 2007, he has been with the School of Electrical Engineering, Royal Institute of Technology, Sweden, where he is currently an Associate Professor in communications theory. He received best paper awards at the International Conference on Wireless Communications and Signal Processing in 2010 and the IEEE International Conference on Computer Communication Networks in 2011. He received the Chinese Government Award for Outstanding Self-Financed Students Studying Aborad in March 2007, the Hans Werthen Grant from the Royal Swedish Academy of Engineering Science (IVA) in March 2006, and Ericsson Research Funding from Ericsson in 2010. Since 2012, he has been an Associate Editor for IEEE TRANSACTIONS ON COMMUNICATIONS, IEEE COMMUNICATIONS LETTERS (Senior Editor Since January 2015) and IEEE WIRELESS COMMUNICATIONS LETTERS.

Guang Yang received the B.E. degree in communication engineering from University of Electronic Science and Technology of China (UESTC), Chengdu, China, in 2010. From 2010 to 2012, he participated in the joint Master-Ph.D. program in the National Key Laboratory of Science and Technology on Communications, UESTC. He joined the Communication Theory Department, Electrical Engineering School, the Royal Institute of Technology (KTH), Stockholm, Sweden, as a Ph.D. student in September 2013.